

# Control of Circularly Polarized Electroluminescence in Induced Twist Structure of Conjugate Polymer

Dong-Myung Lee, Jin-Wook Song, Yu-Jin Lee, Chang-Jae Yu,\* and Jae-Hoon Kim\*

An extremely high degree of circularly polarized photoluminescence (CPPL) and electroluminescence (CEPL) (dissymmetry factor values:  $|g_{\text{PL}}| = 0.72$  and  $|g_{\text{EL}}| = 1.13$ ) are generated from twisted stacking of achiral conjugated polymer induced by nonemitting chiral dopant of high helical twisting power for the first time. Using a theoretical analysis incorporating the Stokes parameter, the twisting angle and birefringence of the aligned conjugated polymer, and the degree of linear polarization in the emitted light are found to make a roughly equal contribution to the degree of CEPL as to the degree of CPPL. Moreover, it is also found that the location of the recombination zone within the emitting layer is a crucial parameter for determining the difference in the dissymmetry factor between CEPL and CPPL. This result is applied to an organic light-emitting display to improve the luminous efficiency by 60%.

The direct emission of circularly polarized (CP) light from conjugated polymers upon photo- or electro-excitation is a key feature for displays, optical data storage, optical quantum information, and chirality sensing.<sup>[1–4]</sup> The CP light can be directly generated by intrinsic material properties used in the light-emitting layer: a helical molecular conformation of luminophores<sup>[5–7]</sup> or a single chiral small molecular emitter.<sup>[8–10]</sup> In the latter case, although it directly emitted high degree of CP light, selection of material is limited and it is necessary to select a host material having suitable characteristics to realize an electroluminescent device.<sup>[8,10]</sup> Therefore, it has been extensively studied about supramolecular helical structure emitting CP light (T1). The intrinsic circular polarized emission can be additionally modulated by extrinsic factors such as differential absorption of emitted CP light (i.e., circular dichroism) or birefringent properties of the material. On the other hand, CP light can also be generated by the propagation of linearly polarized (LP) light through twisted (cholesteric) stacking of birefringent material in macroscopic level (T2).<sup>[11–13]</sup> Although the CP photoluminescence (CPPL) is well established both technically and theoretically,<sup>[13,14]</sup> the understanding of CP electroluminescence (CEPL) is still insufficient, especially in T2. In order to introduce T1 or T2 structures in a nonchiral polymer, there are two main approaches: decorating the light-emitting polymer with chiral pendants (C1)<sup>[5,6,13]</sup> or doping it with

chiral molecules (C2)<sup>[7,11,15]</sup> The degree of circular polarizations is defined by the dissymmetry factor,  $g_{\text{PL or EL}} = 2(I_{\text{L}} - I_{\text{R}}) / (I_{\text{L}} + I_{\text{R}})$ , where  $I_{\text{L}}$  and  $I_{\text{R}}$  denote the intensities of left- and right-handed CP light, respectively. The variables  $g_{\text{PL}}$  and  $g_{\text{EL}}$  represent the dissymmetry factor for PL and EL, respectively.

Since the first demonstration of direct CEPL in a chiral substituted poly(*p*-phenylenevinylene) (PPV) derivative,<sup>[5]</sup> which is categorized as T1/C1, there have been extensive studies within various categories. Liquid-crystalline chiral polyfluorene<sup>[6]</sup> and nonafluorene with varying types and extents of pendant chirality<sup>[13]</sup> have been produced in forms that give rise to T1/C1 and T2/C1 that have  $|g_{\text{EL}}|$  values of 0.15 and 0.35, respectively. In the latter study,<sup>[13]</sup> quantitative analysis of CPPL using CP fluorescence (CPF) theory was attempted, but there was no analysis of CEPL. Since the EL emits light only in the recombination (emission) zone unlike PL, it is necessary to develop the theoretical model for describing CEPL considering the phenomenon. Moreover, the addition of chiral pendants requires a cumbersome synthetic process to control the wavelength of emitted light (i.e., adjusting the color) and the material parameters to maximize the  $g_{\text{EL}}$  value obtained. For a simple and transferable alternative approach, doping achiral light-emitting polymers with a 1-aza[6]helicene molecule<sup>[7]</sup> (i.e., following the C2 approach) has been reported to produce a  $|g_{\text{EL}}|$  value of 0.2, and in this case the direct CEPL origin is T1. Recently, it has been reported that doping lanthanide complex as a chiral emitter produced a very high  $|g_{\text{EL}}|$  value of 1, and discussed the role of position of recombination zone for the high  $g_{\text{EL}}$  value only by considering attenuation of light intensities.<sup>[10]</sup> However, the theory does not describe the phenomenon in the T2 category. Although it has been shown that the T2 structural properties can efficiently implement the CPPL generation in resonance region through the previous studies following the C2 approach,<sup>[11,16,17]</sup> it is not applicable to generate CEPL because it requires micrometer-thick film for the selective reflection.

Here, for the first time, we report and theoretically analyze direct CEPL emissions with the highest value of dissymmetry factor ( $|g_{\text{EL}}| = 1.13$ ) outside the resonance region in twisted stacking of nonchiral conjugate polymer introduced by doping of chiral molecules with high helical twisting power (HTP) (i.e., in the C2/T2 category). We found that the location of the recombination zone within the emitting layer is a crucial parameter for determining the difference in the dissymmetry factor between CEPL and CPPL. The results of this study can

D.-M. Lee, J.-W. Song, Dr. Y.-J. Lee, Prof. C.-J. Yu, Prof. J.-H. Kim  
Department of Electronic Engineering  
Hanyang University  
Seoul 04763, Korea  
E-mail: cjyu@hanyang.ac.kr; jhoon@hanyang.ac.kr

DOI: 10.1002/adma.201700907

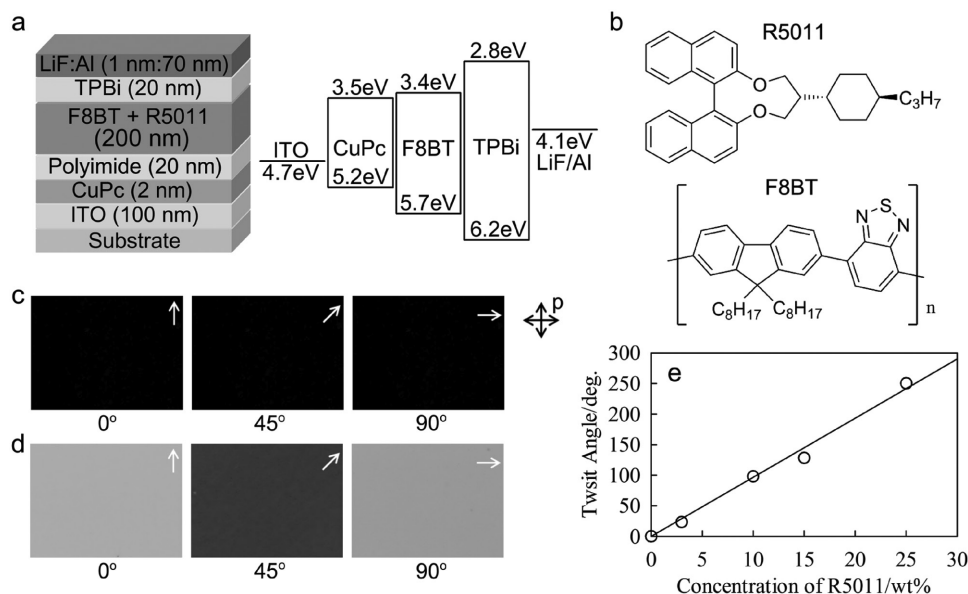


**Figure 1.** a) The schematic diagram of OLED structure and energy levels for the materials used in this study. b) Molecular structure for F8BT and R5011. Microscope textures (100× magnification, Nikon polarizing microscope) with crossed polarizers for the F8BT layer blended with 10 wt% of R5011 c) before thermal annealing and d) after thermal annealing. The arrow indicates the rubbing direction, and the angles represent the angle between the rubbing direction and the axis of the bottom polarizer. e) The twist angle ( $\theta_T$ ) as a function of the blending concentration of R5011. The symbols and solid line represent the experimental and fitted data using  $p^{-1}/(\text{HTP} \times c)$ , respectively.

be used not only to improve the performance of biosensors and optical devices but also to contribute to the improvement of organic light-emitting displays (OLEDs) performance.

We used poly(9,9-di-*n*-octylfluorenyl-2,7-diyl)-*alt*-(benzo[2,1,3]-thiadiazol-4,8-diyl) (F8BT) as our conjugate polymer, doped with a right-handed chiral dopant (R5011) with a high HTP of  $>100 \mu\text{m}^{-1}$ ,<sup>[18]</sup> as an emitting layer (EML). To investigate the effect of the R5011 dopant on the properties of F8BT, we fabricated CP-OLEDs incorporating F8BT with a variety of mixing ratios of R5011 (up to 50%), by spin-coating the EML from toluene solution as part of the EL device structure: indium tin oxide (ITO) (100 nm)/CuPC (2 nm)/polyimide (PI) (20 nm)/F8BT+R5011 (200 nm)/TPBi (20 nm)/LiF:Al (1 nm:70 nm), where CuPC, PI (Al22636), and 2,2',2''-(1,3,5-benzene triyl)-tris(1-phenyl-1-H-benzimidazole) (TPBi) served as the hole injection layer (HIL), rubbed alignment layer (as well as hole transport layer, HTL), and hole blocking layer (HBL), respectively (Figure 1a,b). The PL was obtained from the blend film only on rubbed PI.

No CP light was generated from the pristine films on rubbed PI, regardless of whether the dopant was mixed or not (Figure S1, Supporting Information). This result is different from that obtained in a previous study,<sup>[7]</sup> in which F8BT was doped with 1-aza[6]helicene. In order to find the differences, we observed alignment texture under the polarizing microscope. No difference in texture was observed in the sample before thermal annealing, indicating that the films are isotropic (Figure 1c). However, after quenching to room temperature, followed by thermal annealing at 150 °C above the glass transition temperature ( $T_g = 125 \text{ °C}$ ) for 10 min, we clearly observed uniformly aligned monodomains but different colors at different angles as shown in Figure 1d, which indicates that uniform twisted alignment was achieved by the thermal annealing.

From these results, we suppose that the R5011 did not form a helical molecular conformation of host material, as in previous study,<sup>[7]</sup> but formed a twisted (cholesteric) stacking of host material at the macroscopic level due to a high HTP. We measured the twist angle ( $\theta_T$ ) with various blending concentration of R5011 (Figure 1e), and obtained a  $\text{HTP} = 13.4 \mu\text{m}^{-1}$  by fitting the data with  $p^{-1}/(\text{HTP} \times c)$  where  $p$  and  $c$  are the pitch of the twisted stacking and concentration of the dopant, respectively. This low HTP value of the F8BT relative to that of a small-molecule LC ( $>100 \mu\text{m}^{-1}$ ) may be due to the higher molecular weight and elastic constant of F8BT, and the stronger surface anchoring energy of the thin F8BT. Considering that chiral dopants with a  $\text{HTP} \approx 10 \mu\text{m}^{-1}$  are generally used for cholesteric arrangement in LCs,<sup>[18]</sup> the HTP value for F8BT is reasonable for introducing twisted stacking in the F8BT layer. It was thus concluded that the twisted stacking of F8BT is introduced by R5011 due to a high HTP, and it may play a predominant role over the helical molecular conformation for CP light generation. It is note that OLEDs need to remain stable when stored at a temperature of 85 °C for extended periods of time in many commercial applications. It is also important that the twisted structure be maintained at a high temperature since the temperature of the device may rise by more than 20 °C by joule heating when driving the OLED.<sup>[19]</sup> Since the F8BT used in this study has a nematic phase of 120 °C or more, the twisted structure is maintained even when the temperature rises to 100 °C (Figure S2, Supporting Information).

Figure 2 shows the CPPL and CPEL spectra and calculated  $g$  values obtained from the blend film with 10 wt% of R5011 and pure F8BT film without a dopant on rubbed or unrubbed alignment layer. Bright CPEL emission, achieving 4000  $\text{cd m}^{-2}$ , was measured for a blend sample with an efficiency of 4.46  $\text{cd A}^{-1}$  (Figure S3, Supporting Information). Even

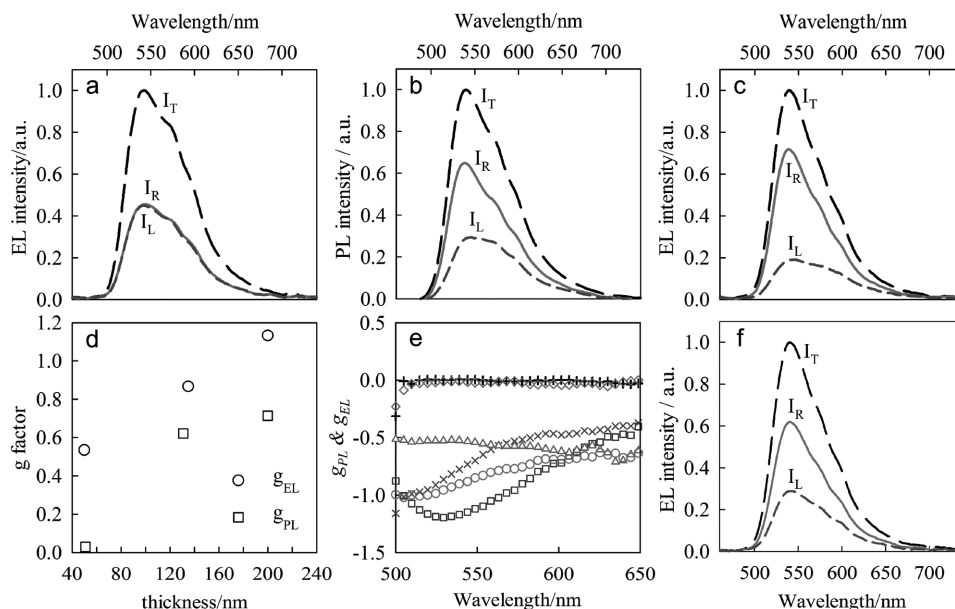


**Figure 2.** a) CPEL spectra for the pure F8BT film ( $d = 200$  nm) without dopant. The intensities measured without a circular polarizer, and with right- and left-handed circular polarizers are presented by long dashed ( $I_T$ ), solid ( $I_R$ ), and short dashed ( $I_L$ ) lines, respectively. For the comparison, the intensities were normalized with respect to the peak intensity without a circular polarizer. b) CPPL and c) CPEL spectra for blended F8BT film ( $d = 200$  nm) with 10 wt% of R5011. d) Thickness dependence of  $|g_{PL}|$  and  $|g_{EL}|$ . e)  $g_{PL}$  (+ and  $\times$  symbols derived from CPPL spectra for the pure F8BT film and (b), respectively) and  $g_{EL}$  (diamond and square symbols derived from (a) and (c), respectively) for  $d = 200$  nm. The  $g_{EL}$  values for  $d = 50$  (triangle) and 135 nm (circle) were calculated from Figure S5 (Supporting Information). f) CPEL spectra for the blend F8BT film on unrubbed polyimide.

after thermal annealing, unsurprisingly, CPEL light emitted from pure F8BT was equivalent in intensity across the entire range of measured wavelength whether measured with a left- or right-handed CP filter (Figure 2a). CPPL also showed the same result. On the other hand, pure F8BT on rubbed PI generated LP light of  $P_{PL} = 0.891$  and  $P_{EL} = 0.875$  at  $\lambda = 546$  nm, where  $P$  is a degree of linear polarization, and  $I_R:I_L = 1:1$  (i.e.,  $g_{EL} = 0$ ). However, the  $g_{PL}$  and  $g_{EL}$  values were dramatically increased to  $-0.72$  and  $-1.13$  at  $\lambda = 546$  nm in the sample with chiral dopant (Figure 2b,c).

It is evident from this dramatic increase that the LP light generated by the F8BT layer becomes CP light as it travels through the twisted stacking of the birefringent F8BT. Therefore, the location and range of the recombination (emission) zone, the birefringence of the film and the degree of linear polarizations are important for CPEL generation.

Note that the  $g_{PL}$  and  $g_{EL}$  values for F8BT with S isomer (i.e., S5011) show equal and opposite sign within error bound (Figure S4, Supporting Information). It means that left- or right-handed twisted stacking of F8BT is introduced depending on the chirality of dopants. Another point to note is that an elliptically polarized (EP) light, in general, is generated when LP light propagates a twisted stacking of conjugate polymer depending on the layer thickness, birefringence of polymer, and wavelength of emitted light. The EP light can be thought of as combinations of left- and right-handed circular components of unequal amplitude.<sup>[20]</sup> The calculated  $g$  value after separating into two circularly polarized light from EP light with considering random polarization by partially polarized light emission ( $P_{PL} = 0.891$  and  $P_{EL} = 0.875$  at  $\lambda = 546$  nm) is almost equal to the experimentally measured  $g$  value within error bound

(see the Supporting Information for further details, Figure S5, and Table S1, Supporting Information). It means that the  $g$  value can be calculated from the light intensity measurement with left- and right-handed circular polarizer as we did in this study, even though it includes RP component. With considering that it is hard to realize the generation of fully polarized light even in well-ordered conjugate polymer, the generation of RP is unavoidable in T2 category. Moreover, since it is important to consider overall degree of CP light when implementing a device with emitting CP light such as OLEDs, we measured  $g$  values including the effect of RP in this study.

Figure 2d shows the thickness dependence of  $g$  values also indicating that the origin of the CP light is in category T2 (see Figure S6, Supporting Information, for CPPL and CPEL spectra). Although the thickness between 50 and 135 nm is commonly used for the fabrication of conventional polymer OLEDs, we fixed the thickness of the blend film at 200 nm in further study to characterize the effect of the recombination zone. Indeed, the values of  $g_{EL}$  obtained with  $d = 50$  nm were generally constant across the emission spectra as shown in Figure 2e, but this was not the case of  $d = 200$  nm suggesting that the  $g_{EL}$  values were greatly affected by the retardation ( $\Delta n \cdot$  optical pass length, where  $\Delta n$  is birefringence of F8BT layer) of the consisting material. Higher value of  $g_{EL}$  compared to  $g_{PL}$ —despite lower  $P$  values of EL compared to PL—also suggests a narrower emission zone near the HBL/EML interface for EL than PL, at the same thickness. Note that the F8BT blend on unrubbed PI shows  $g_{PL} = -0.46$  and  $g_{EL} = -0.71$ , which are still sufficiently high with respect to other studies (Figure 2f). These results indicated that the presence of monodomain in the film is not critical for CP light generation, because the twisted

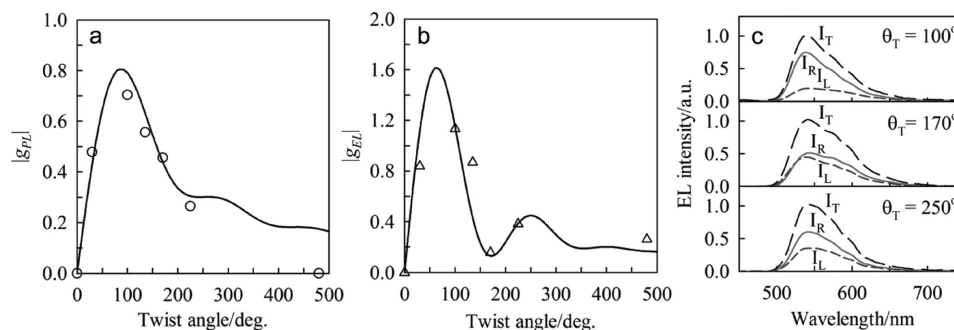


**Figure 3.** a)  $|g_{PL}|$  and b)  $|g_{EL}|$  as a function of  $\theta_T$  for the sample of  $d = 200$  nm. The symbols are experimentally acquired values from the CPPL and CPEL spectra, and the solid lines are corresponding calculated values using the Mueller matrix method. For the calculation, we used  $P_{PL} = 0.891$  and  $P_{EL} = 0.875$  for PL and EL, respectively,  $\Delta n = 0.67$  at  $\lambda = 546$  nm from ref. [21] and  $d = 200$  nm. c) CPEL spectra for the sample with  $\theta_T = 100^\circ$ ,  $170^\circ$ , and  $250^\circ$ .

stacks within a polydomain contribute equally and in the same way as a monodomain film as a whole, in terms of the observed  $g_{PL}$  or  $g_{EL}$ . Since the rubbing of thin layer in OLEDs can have a significant effect on the display performance, this result is very important in practical applications.

In order to study the effect of twist angle ( $\theta_T$ ) on the  $g_{PL}$  and  $g_{EL}$ , we controlled the concentration of R5011.  $|g_{PL}|$  increased with increasing  $\theta_T$  up to  $90^\circ$ , and then gradually decreased with further increases of  $\theta_T$  (Figure 3a). Interestingly, the  $|g_{EL}|$  showed peculiar behavior of sudden drop around  $\theta_T = 170^\circ$  (Figure 3b). Figure 3c represents the CPEL spectra for the sample with  $\theta_T = 100^\circ$ ,  $170^\circ$ , and  $250^\circ$ . It is very clear that the difference of the intensities passing through left- and right-handed circular polarizer diminishes at  $\theta_T = 170^\circ$ . To confirm whether this abnormal behavior was due to an artificial effect or an intrinsic property of our system, we calculated the  $g$  value from Stokes parameters ( $|g| = 2S_3/S_0$  where  $S_0$  and  $S_3$  are Stokes parameters for describing light intensity, and handedness and degree of circular polarization, respectively) applying the Mueller matrix for the twisted birefringent material<sup>[22]</sup> (see the Supporting Information for further details on  $g$  calculation). From the calculations, it was derived that  $g = Pg_f$  when partially polarized light (i.e.,  $P < 1$ ) passed through the twisted stacking of conjugate polymer, where  $g_f$  is the dissymmetry factor for fully polarized LP light (i.e.,  $P = 1$ ).

For the calculation, we divided the film into ten sublayers of 20 nm, and assumed that F8BT is uniformly twisted in the film and the twist angle ( $\theta_i = \theta_T z_i/d$  where  $\theta_i$ ,  $\theta_T$ ,  $z_i$ , and  $d$  are the twist angle of  $i$ th sublayer, total twist angle, distance from the HBL layer, and thickness of the film, respectively) is fixed in each sublayer. In the case of PL, every sublayer absorbs the UV light and emits LP light along the twist angle ( $\theta_i$ ) in each layer ( $z = z_i$ ) simultaneously, and the LP light propagate through the rest of the sublayers (Figure 4a). The final  $g$  value was calculated by averaging the  $g$  values from the light generated in each sublayer. We supposed that the intensity of the excited UV light was the same in all sublayers, and there was no intensity attenuation. The solid line in Figure 3a represents the calculated  $|g_{PL}|$  values with  $P_{PL} = 0.891$ , which describes the experimental data well. Our approach also corresponds well with the results of ref. [13] in which nonfluorene exhibited varying extent of pendants chirality (see the Supporting Information and Figure S7, Supporting Information).

On the other hand, in the case of EL, since the LP light is emitted only in the recombination zone in both directions toward the anode and the cathode unlike PL, reflection at the cathode must be considered (Figure 4b)—half of the emitted LP light from the recombination zone propagated to the anode (ITO), and the other half propagated to the cathode (LiF/Al), where the light was reflected and repropagated in all of the sublayers. The  $g_{EL}$  values were calculated by averaging the  $g_{EL}$  values for both directions. To identify the location of the recombination zone for EL, we plotted the contour map of the calculated  $g$  values for light emission in each sublayer as a function of  $\theta_T$  in Figure 4c. The degree of CPEL increased when the recombination zone became closer to  $z = 0$  (i.e., closer to the F8BT/TPBi interface) within a range of  $\theta_T$  of  $30^\circ$ – $100^\circ$ , and showed local minima at certain  $\theta_T$  value. In order to compare with experimental result (Figure 3b), we presented the  $|g_{EL}|$  profiles for light generated at  $z = 0$ , 20, and 100 nm from the HBL layer as a function of  $\theta_T$  in Figure 4d (see Figure S8, Supporting Information, for different thickness). Since the optical path length to the cathode was longer than to the anode, except the emission at  $z = 0$ , the beam incurred higher retardation, and  $|g_{EL}|$  values have minima at shorter periods. Although the  $|g_{EL}|$  profile for the light generated at  $z = 100$  nm cannot explain the peculiar behavior around  $\theta_T = 170^\circ$ , the results of  $z = 0$  and 20 nm describe the phenomena well. It has been reported that the recombination zone for EL extends over a 40 nm distance in the EML,<sup>[23]</sup> and a proper interlayer between the EML and electrode can control the location of the recombination zone.<sup>[24]</sup> Because the TPBi layer between the cathode and EML acts as a HBL in our OLEDs, the injected holes from the anode were accumulated at the EML/HBL interface, and, as a result, we conclude that the recombination zone was located near the interface. This conclusion is confirmed by the decrease in  $g_{EL}$  upon removal of the HIL (CuPC) layer—the resulting decrease in hole injection would have decreased the number of accumulated holes at the interface, and the recombination zone would therefore have moved away from the interface (Figure S9, Supporting Information). Therefore, we can assume that the recombination zone can be extended to 40 nm from the TPBi layer in our system. The solid line in Figure 3b represents the average of the  $|g_{EL}|$  profiles at  $z = 0$ , 20, and 40 nm, and well describes the abnormal behavior of the  $g_{EL}$  values. For the calculation, we used  $\Delta n = 0.67$  at  $\lambda = 546$  nm,  $P_{EL} = 0.875$ , and  $d = 200$  nm. In

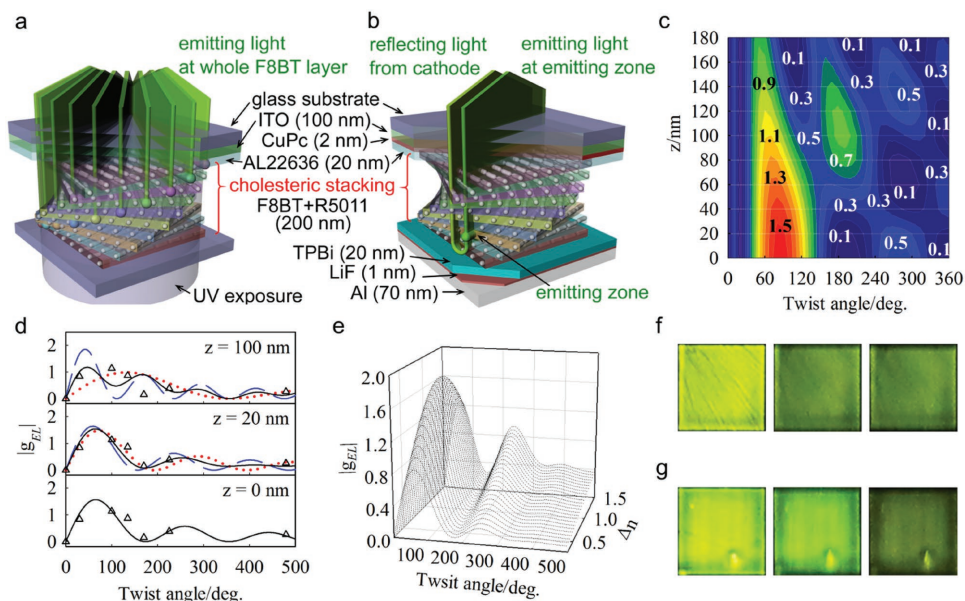


**Figure 4.** Schematic diagrams of the twisted stacking of rigid rods describing F8BT molecules in a sublayer with a thickness of  $d$  for the a) CPPL and b) CPEL calculations. c) Contour map of the calculated  $|g_{EL}|$  as a function of the twist angle ( $\theta_T$ ) and the location of the recombination zone ( $z$ ). The numbers are values of the  $|g_{EL}|$  factor. The guide lines of the  $y$ -axis represent the location of the recombination zone. d) Calculated  $|g_{EL}|$  as a function of the twist angle ( $\theta_T$ ) at different recombination zone of 0, 20, and 100 nm. e) Calculated  $|g_{EL}|$  values as a function of the twist angle ( $\theta_T$ ) and birefringence ( $\Delta n$ ). We supposed that the light was emitted at  $z = 0$ ,  $P_{EL} = 0.875$ , and  $d = 200$  nm. Photographs for OLED samples with f) pure F8BT on unrubbed PI and g) doped F8BT with 10 wt% of R5011 on rubbed PI. We adjust the voltage to generate a consistent intensity of EL for the comparison. The first, second, and third photographs were taken under no polarizer, a right-handed, and a left-handed circular polarizer, respectively. The intensities of the samples are summarized in Table S2 (Supporting Information).

Figure 4e, we represent the calculated  $|g_{EL}|$  values as a function of material parameters such as the twist angle ( $\theta_T$ ) and birefringence ( $\Delta n$ ). The  $|g_{EL}|$  increased with increasing  $\Delta n$  up to 1 and subsequently decreased. From the results, we obtained almost pure CPEL under conditions of  $\Delta n = 0.95$  and  $\theta_T = 60^\circ$  for  $d = 200$  nm.

Because conventional OLEDs emitting unpolarized light use a circular polarizer to prevent reflection of ambient light,<sup>[25]</sup> the maximum light efficiency of the emitted light is about 50% when other losses such as internal reflection are not taken into account. However, direct emission of CP light in OLEDs with the same handedness as laminating circular polarizer can increase the efficiency of the emitted light (Figure S10, Supporting Information). Figure 4f,g shows photographs of OLED pixel for pure F8BT on unrubbed PI and doped F8BT on rubbed PI under left- and right-handed circular polarizers, respectively (see Table S2, Supporting Information, for measured intensities of the samples). It can be clearly seen that the case of emitting CP light with the same handedness as circular polarizer is the brightest. The obtained dissymmetry factor  $|g_{EL}|$  of 1.13 reported here is sufficient to induce about 60% increase in brightness compared to nonpolarized conventional OLEDs using a circular polarizer.

In summary, for the first time, extremely high degree of circular polarization in PL and EL (dissymmetry factor values:  $|g_{PL}| = 0.72$  and  $|g_{EL}| = 1.13$ ) are generated from twisted stacking of achiral conjugated polymer induced by nonemitting chiral dopant of high helical twisting power. Our quantitative results suggest that the key features for obtaining a high  $g$  value in PL and EL light from a twisted stacking system are the retardation and twist angle

of the emitting layer, and degree of the linear polarization from the emitted light. Furthermore, the location of the recombination (emission) zone within the emitting layer is a crucial parameter for determining the difference in the dissymmetry factor between CPEL and CPPL. This result may help to determine the molecular synthesis approaches as well as the design of the device structure that will generate almost pure CP light from EL or PL.

## Experimental Section

**Materials:** The conjugate polymer, F8BT (molecular weight = 70 000), was commercially acquired from LUMTEC. F8BT has a nematic LC phase over  $T = 125^\circ\text{C}$ , and an absorption peak at 460 nm for film. The right-handed chiral dopant, R5011, was commercially acquired from Merck, with a high HTP value of  $>100\ \mu\text{m}^{-1}$  for small-molecule LCs. Due to such a high HTP, R5011 was used to induce a blue phase in LC.<sup>[18]</sup> However, the HTP value can change according to the molecular weight and elastic properties of the host materials.

**Fabrication of OLEDs:** F8BT was dissolved with a variety of mixing ratios of R5011 (3, 10, 15, 20, 25, and 50 wt%) in toluene for spin-coating. Prepatterned ITO substrates with a sheet resistance of  $\approx 20\ \Omega\ \text{sq}^{-1}$  were rinsed in an ultrasonic bath with deionized water and mucasol (alkali detergent) for 60 min. Copper phthalocyanine (CuPC) with thickness of 2 nm was commercially acquired from LUMTEC, and was deposited by high-vacuum ( $6 \times 10^{-6}$  torr) thermal evaporation for hole injection on ITO. An AL22636 PI, commercially acquired from JSR, was used as an alignment layer for the EML as well as a HTL. The AL22636 PI was spin-coated on the CuPC layer, and unidirectionally rubbed by a rubbing machine with a 6.5 cm diameter roller covered with cotton cloth. The dissolved F8BT blend in toluene ( $28.7\ \text{mg mL}^{-1}$ ) for 200 nm thickness was spin-coated at 3000 rpm for 20 s followed by 1000 rpm for 10 s on rubbed PI. After that, TPBi (20 nm), LiF (1 nm),

and Al (70 nm) were deposited by high-vacuum ( $6 \times 10^{-6}$  torr) thermal evaporation as an HBL to confine excitons in the EML, electron injection layer, and cathode, respectively. All EL samples were encapsulated by glass and an optical UV curable resin (NOA 65) to avoid exposure to humidity and oxygen. The schematic diagrams of the OLED structure, and energy levels of the used materials are shown in Figure 1a,b.

**Methods:** Left- and right-handed CP emission spectra from the blended thin films were collected using a linear polarizer and quarter-wave plate placed before an Ocean Optics USB2000 spectrometer. EL was adjusted by applying voltages in the range of 10–11 V in order to generate consistent intensity of the emitted light. For PL, a UV light source (365 nm) was emitted with an intensity of 1000 W. The current density ( $J$ )–voltage ( $V$ )–luminance ( $L$ ) characteristics of the OLEDs were evaluated using a source meter (Keithley 2400, Keithley Instruments Inc.) and a luminance meter (CS-1000, Konica Minolta, Japan). The spectra of polarized light were measured using a spectrometer (USB-2000, OceanOptics). The twist angle was determined by direct measurement of the Stokes parameters of the transmitted light described in ref. [26].

## Supporting Information

Supporting Information is available from the Wiley Online Library or from the author.

## Acknowledgements

This work was supported by KDRC (Korea Display Research Consortium) support program for the development of future devices technology for display industry.

## Conflict of Interest

The authors declare no conflict of interest.

## Keywords

circular polarization, conjugate polymers, electroluminescence, organic light-emitting displays, recombination zones

Received: February 14, 2017

Revised: April 17, 2017

Published online:

- [1] R. Singh, K. N. Unni, A. Solanki, Deepak, *Opt. Mater.* **2012**, *34*, 716.
- [2] C. Wang, H. Fei, Y. Qiu, Y. Yang, Z. Wei, Y. Tian, Y. Chen, Y. Zhao, *Appl. Phys. Lett.* **1999**, *74*, 19.
- [3] C. Wagenknecht, C.-M. Li, A. Reingruber, X.-H. Bao, A. Goebel, Y.-A. Chen, Q. Zhang, K. Chen, J.-W. Pan, *Nat. Photonics* **2010**, *4*, 549.
- [4] Y. Yang, R. C. da Costa, M. J. Fuchter, A. J. Campbell, *Nat. Photonics* **2013**, *7*, 634.
- [5] E. Peeters, M. P. T. Christiaans, R. A. J. Janssen, H. F. M. Schoo, H. P. J. M. Dekkers, E. W. Meijer, *J. Am. Chem. Soc.* **1997**, *119*, 9909.
- [6] M. Oda, H.-G. Nothofer, G. Lieser, U. Scherf, C. J. Meskers, D. Neher, *Adv. Mater.* **2000**, *12*, 362.
- [7] Y. Yang, R. C. da Costa, D.-M. Smilgies, A. J. Campbell, M. J. Fuchter, *Adv. Mater.* **2013**, *25*, 2624.
- [8] F. Zinna, U. Giovanella, D. Bari, *Adv. Mater.* **2015**, *27*, 1791.
- [9] J. R. Brandt, X. Wang, Y. Yang, A. J. Campbell, M. J. Fuchter, *J. Am. Chem. Soc.* **2016**, *138*, 9743.
- [10] F. Zinna, M. Pasini, F. Galeotti, C. Botta, L. D. Bari, U. Giovanella, *Adv. Funct. Mater.* **2017**, *27*, 1603719.
- [11] S. H. Chen, D. Katsis, A. W. Schmid, J. C. Mastrangelo, Y. Tsutsui, T. N. Blanton, *Nature* **1999**, *397*, 506.
- [12] M. R. Craig, P. Jonkheijm, S. Meskers, A. Schenning, E. W. Meijer, *Adv. Mater.* **2003**, *15*, 1435.
- [13] Y. Geng, A. Trajkovska, S. W. Culligan, J. J. Ou, H. Chen, D. Katsis, S. H. Chen, *J. Am. Chem. Soc.* **2003**, *125*, 14032.
- [14] H. Shi, B. M. Conger, D. Katsis, S. H. Chen, *Liq. Cryst.* **1998**, *24*, 163.
- [15] S. Haraguchi, M. Numata, C. Li, Y. Nakano, M. Fujiki, S. Shinkai, *Chem. Lett.* **2009**, *38*, 254.
- [16] M. Voigt, M. Chambers, M. Grell, *Chem. Phys. Lett.*, **2001**, *347*, 173.
- [17] A. Y. Bobrovsky, N. I. Boiko, V. P. Shibaev, J. H. Wendorff, *Adv. Mater.* **2003**, *15*, 282.
- [18] Y. Chen, S.-T. Wu, *J. Appl. Polym. Sci.* **2014**, *131*, 40556.
- [19] F. A. Boroumand, A. Hammiche, G. Hill, D. G. Lidzey, *Adv. Mater.* **2004**, *16*, 252.
- [20] D. S. Kliger, J. W. Lewis, C. E. Randall, *Polarized Light in Optics and Spectroscopy*, Academic Press, New York **1990**, Ch. 2.
- [21] M. Campoy-Quiles, P. G. Etchegoin, D. D. C. Bradley, *Phys. Rev. B* **2005**, *72*, 045209.
- [22] D.-K. Yang, S.-T. Wu, *Fundamentals of Liquid Crystal Devices*, John Wiley & Sons, Chichester, UK **2006**, Ch. 3.
- [23] J. Griener, M. Remmers, D. Neher, *Adv. Mater.* **1997**, *9*, 964.
- [24] J.-S. Kim, R. H. Friend, I. Grizzi, J. H. Burroughes, *Appl. Phys. Lett.* **2005**, *87*, 023506.
- [25] G. Trapani, R. Pawlak, G. R. Carlson, J. N. Gordon, *US Patent 6549335* **2003**.
- [26] Y. Zhou, Z. He, Z. S. Sato, *Jpn. J. Appl. Phys.* **1997**, *36*, 2760.